

STRUCTURE AND PROPERTIES OF CRYSTALLINE INCLUSIONS ENTRAPPED IN MINERALS

MARTA MORANA

Dipartimento di Scienze della Terra e dell'Ambiente, Università di Pavia, Via Adolfo Ferrata 1, 27100 Pavia

INTRODUCTION

Mineral inclusions are formed by minerals trapped within larger crystals during either their formation or their re-crystallization. Inclusions are ubiquitous in rocks, since any mineral can in principle trap and preserve the phases present in their growth environment. From the moment of their entrapment, inclusions are isolated from most of the physico-chemical changes affecting rocks at depth and can thus provide insights about the formation of the host crystal, the protoliths and P-T paths of metamorphic rocks. This thesis is focused on two large groups of inclusions: inclusions in diamond and inclusions in metamorphic rocks.

Since diamond is chemically inert, the inclusions within are protected and can reach unaltered the Earth's surface. Therefore, mineral inclusions in diamond provide pristine samples from regions of the Earth that we cannot access directly, over a wide range of geological times. Thus, it is not surprising that studies on mineral inclusions in diamonds have played a fundamental role in our understanding of where and when their diamond hosts form. In fact, a key aspect of diamond inclusions studies is the time of formation of the inclusions with respect to the diamond host. Inclusions are classified as protogenetic, syngenetic or epigenetic, whether their formation preceded, accompanied or followed crystallization of their host diamonds. The traditional criterion to identify the time of formation is the observation of the morphology of the included crystals. In fact, inclusions showing a cubo-octahedral morphology, irrespective of their crystal system, were thought to grow at the same time as diamond, which could impose its morphology. Analogously, protogenetic inclusions were supposed to show a shape determined by their own crystal system. Since its introduction in the late Sixties, the use of the electron microprobe allowed to conduct a systematic characterization of inclusions in diamond, including the compilation of large databases (Stachel & Harris, 2008), and to estimate the conditions of pressure and temperature of last equilibration from non-touching pairs of different mineral species included in diamond. However, these well-established approaches have recently shown some limitations. Firstly, the imposition of morphology has been proven to fail in the case of olivine inclusions that were identified as protogenetic, despite their cubo-octahedral morphology (Nestola *et al.*, 2014; Milani *et al.*, 2016). Furthermore, geothermobarometric estimates rely on the occurrence of certain mineral pairs assumed to be in equilibrium, and require the extraction of the inclusions from the diamond host. On the contrary, non-destructive techniques can be applied to have further insights on the time and conditions of formation of the host-inclusions pair. Tomographic analyses can detect the presence of fractures that suggest a late alteration for the inclusions, whereas X-ray diffraction can identify not only the minerals comprising the inclusions, but also epitaxial growth relationships between the inclusions and the host diamond through crystallographic orientation relationships (Milani *et al.*, 2016; Nimis *et al.*, 2019). Elastic geobarometry represents a non-destructive alternative to chemical thermobarometry. In this methodology, the difference in elastic properties between the host and the inclusion is used to derive the entrapment pressure and can be applied also to monomineralic inclusions, since it does not rely on the assumption of equilibrium between mineral pairs.

Diamonds do not only grow in deep Earth, but can also form as a result of meteorite impacts on the Earth's surface, or occur as presolar dust grains of interstellar origin, and as component of meteorites, such as ureilites. The formation process of diamond in these meteorites is still unclear and three main hypotheses are debated: growth under static high-pressure conditions, shock origin, or formation by chemical vapor deposition. These hypotheses are discussed in this thesis as a peculiar case in diamond studies.

Most of the considerations about diamond inclusions apply also to the study of metamorphic rocks, where inclusions play a fundamental role, in particular in the case of the so-called ultrahigh-pressure metamorphism.

In this context, mineral inclusions can be of great interest, since they can provide insights on the condition of pressure, temperature and depth in which the host grew. As in the case of diamond inclusions, the composition of inclusions trapped during growth have long been used to derive pressure and temperature conditions, but elastic geobarometry is emerging as an alternative method that does not require equilibrium between the minerals, but relies on difference in elastic properties.

INCLUSIONS IN DIAMONDS

Diamond is among the most studied materials, due to its physical properties, but natural diamonds have further geological relevance since they provide extraordinary information from the deepest, and otherwise inaccessible, regions of our planet. In fact, natural diamonds can contain mineral inclusions that were trapped during their formation at depth and act as windows on the Earth's interior, providing fundamental insights on the composition of the deep Earth and global geo-dynamics. As such, the study of inclusions in diamonds is crucial to improve our understanding of the formation and evolution of the solid Earth through geological times and, as a consequence, the geological processes shaping the Earth's surface and impacting the environment. Furthermore, inclusions entrapped at different times provide information on various time scaling, related to distinct growth conditions and environments. In this context, iron oxides inclusions are potentially of great interest, because of their iron content that could be used to infer the oxygen fugacity conditions in which they grew (McCammon *et al.*, 1997), but they are rare and often difficult to classify in terms of both time of formation and paragenesis. Magnetite ($\text{Fe}^{2+}\text{Fe}^{3+}_2\text{O}_4$), in particular, is a rare inclusion of unknown paragenesis, that has been found in various localities worldwide.

This study was focused on a suite of 14 diamonds from the Judith Milledge collection, originally obtained from Consolidated African Selection Trust (CAST), the major mining company in Ghana from 1924 to 1972 operating in Akwatia, Birim river valley. The diamonds have size ranging from 0.5 to 2 mm, with slightly octahedral or irregular shapes. The samples were characterized using a combination of non-destructive techniques: X-ray diffraction, Raman spectroscopy, magnetometry and synchrotron-based X-ray tomographic microscopy.

Five diamonds (CAST2-2, -3, -5, -14, -15) contained inclusions consisting of a mixture of polycrystalline magnetite and hematite (Fe_2O_3); in some cases it was not possible to distinguish between magnetite and magnesioferrite ($\text{MgFe}_3^{+2}\text{O}_4$), since they have the same space group ($Fd3m$, No. 227), similar lattice parameters and chemical composition, but it has been shown that magnetic properties can guide the identification (Piazzini *et al.*, 2019). In fact, the volume of the inclusion calculated from the tomographic scan can be used to predict the saturation magnetization associated to that volume of magnetite or magnesioferrite, through the relationship $M_{sat} = m_{sat}/V_{mag}$, where M_{sat} is the saturation magnetization, m_{sat} is the experimentally determined magnetic moment and V_{mag} is the volume of the magnetic inclusion obtained from the segmentation of the tomographic data. Then, the calculated value can be compared with reported values of M_{sat} to identify the composition of the inclusion. However, this method can only be applied when there is only one magnetic inclusion in the host. A careful inspection of the SRXTM images of these samples clearly show that inclusions containing hematite are all connected to the surface by fractures, suggesting that this inclusion is most probably an epigenetic product. This is not surprising considering the high oxidation state of Fe in this mineral that indicate relatively oxidizing conditions. Sample CAST2-11 is of particular interest since it contains only one inclusion that was found to comprise a mixture of magnetite and quartz. Strikingly, this diamond does not show any fractures and the inclusion is completely trapped within the host. This occurrence is similar to the previously described magnetite inclusions from Madwui, Tanzania (Stachel *et al.*, 1998) that showed a distribution of silica resulting from the exsolution from a magnetite that was originally homogeneous and high in SiO_2 . The experimental results by Woodland & Angel (2000) could provide an explanation for the occurrence of such sample, since they showed that significant solid solution of Fe_2SiO_4 in magnetite can indeed occur at moderate pressures and temperatures. Considering this, the silica lamellae could have been originated through exsolution of Fe_2SiO_4 in magnetite due to decompression.

Diamonds in ureilites

The presence of diamonds in ureilites, the second largest group of achondrites, was reported more than a century ago, but the process by which the diamonds formed is still unclear. Three main hypotheses are taken into account: growth under static high-pressure conditions in the interior of large meteorite parent bodies, formation by shock conversion of graphite, or at low pressure in the solar nebula by chemical vapor deposition. Recent work on the Almahata Sitta (AhS) polymict ureilite by Miyahara *et al.* (2015) and Nabiei *et al.* (2018) reported the presence of large diamonds with inclusions of chromite and Fe-S-P phases and suggested that such diamonds could only be formed at static pressures higher than 20 GPa, implying the existence of a parent body similar in size to Mercury or Mars Nabiei *et al.* (2018). To provide insight into the origin of diamonds in ureilites, carbon phases in two ureilitic stones from AhS, samples AhS 209b and AhS 72, and also the NWA7983 main group ureilite were investigated by single-crystal micro X-ray diffraction (XRD), micro-Raman spectroscopy, and Transmission Electron Microscopy. The combined results from these three techniques suggest that the most likely process by which both microdiamonds and nano-diamonds in ureilites formed is in a shock event characterized by a peak pressure possibly as low as 15 GPa, that is the shock level recorded by the silicates present in the samples. Micrometer-sized diamonds can form from crystalline graphite in shock events when catalyzed by metallic Fe-Ni-C liquid, which was present during the major shock events that occurred on the parent body, and do not require high static pressures and long growth times. None of the minor Fe-S-P phases associated with the diamonds in ureilites require high static pressures either, thus the results suggest that there is no evidence that diamonds in ureilites formed in large planetary bodies or planetary embryos.

INCLUSIONS IN METAMORPHIC ROCKS

Quartz is by far one of the most common mineral inclusions in different types of rocks such as sandstones, granites, granodiorites, rhyolites and metamorphic rocks. It can be trapped as an inclusion in garnets during the prograde metamorphism and the growth of the host crystal. This host-inclusion pair has recently emerged as a promising candidate for elastic geobarometry applications to back-calculate the pressure and temperature conditions at the entrapment of the inclusions mineral (Murri *et al.*, 2018; Gonzalez *et al.*, 2019; Mazzucchelli *et al.*, 2019; Alvaro *et al.*, 2020). Moreover, the thermoelastic properties of quartz have been thoroughly characterized by means of X-ray and neutron diffraction, Raman and Brillouin spectroscopy, and computational techniques, thus providing basis and reference data for elastic geobarometry.

X-ray diffraction study of a quartz inclusion in garnet

The crystal structure of mineral inclusions has rarely been characterized *in situ* (Ikuta *et al.*, 2007). This is indeed an interesting case, since the included mineral, being entrapped inside another crystal, is not under hydrostatic stress conditions, as a result of the difference in the elastic properties of the two crystals and their mutual crystallographic orientations. Till now information on the effect of deviatoric stress on the structure of quartz were limited to Density Functional Theory (DFT) calculations that showed that non-hydrostatic conditions affect mostly the internal angular deformation of the SiO₄ tetrahedra, whereas have little influence on the tilts and volume of the tetrahedra (Murri *et al.*, 2019). Considering the ubiquity of quartz in rocks and the large amount of information available on its structure and properties, quartz inclusions in garnet represent an ideal starting point to characterize the structure of minerals under non-hydrostatic conditions and can potentially provide a better understanding of the stress conditions phenomena occurring at depths, such as subduction and metamorphic events. To understand the effect of the confinement within the host, the bond distances and angles obtained from the inclusion were compared with the ones from a free crystal refinement performed with the same parameters used for the inclusions. The bond lengths in the two datasets, are the same within the esd's, whereas the angles show a larger variation. This is not surprising, since compression mostly affects the Si-O-Si angle, while the Si-O change only slightly (Glinnemann *et al.*, 1992). As a further test, the experimental results can be compared with the DFT calculation by. For the same strain conditions calculated from the unit cell parameter, the Si-O-Si angle, which is

the most affected angle by deviatoric stress, varies of 2.2° that is in good agreement with the value of $2.3^\circ(6)$ obtained from the inclusion data. In addition, the O2-Si-O3 and O4-Si-O5 angles show a variation of 0.25° and 0.20° in computational and experimental data respectively. The O2-Si-O5 and O3-Si-O4 angles also show the same pattern.

Raman spectroscopy for elastic geobarometry: quartz in garnet as a case study

Elastic geobarometry exploits the difference in elastic properties of host-inclusion pairs to back-calculate the entrapment pressures for the inclusions, P_{trap} , starting from their residual or remanent pressure, P_{inc} , measured when the host is at room conditions. For this application, Raman spectroscopy is a popular technique, since it is quick and allows small portions of the sample to be probed, thus providing information about the variation of the stress and strain inside the analyzed inclusions. Assuming that the inclusions are under hydrostatic pressure, the residual pressure can be determined from the shift of the Raman modes with respect to a free quartz crystal (Enami *et al.*, 2007), applying a hydrostatic calibration such as the one provided by Schmidt & Ziemann (2000). The main issue with this approach is the assumption of hydrostaticity. In fact, due to the inherent elastic anisotropy of crystals, the inclusion-host boundary imposes deviatoric stress on any mineral trapped even in a cubic host, and, in particular for non-cubic mineral inclusions, the deviation from hydrostaticity may be considerable. Since the variation in the Raman peak positions of a crystal results from the strain imposed on it (Angel *et al.*, 2019) an inclusion crystal will have different Raman shifts with respect to a crystal under hydrostatic pressure. Indeed, a recent experimental study by Bonazzi *et al.* (2019) has demonstrated that the values of P_{inc} and P_{trap} obtained from the hydrostatic calibration are not reliable when the strains imposed on the inclusions are significantly different from those of a crystal under hydrostatic conditions. For quartz inclusions, the strains can be calculated from the measured Raman shifts by using the phonon-mode Grüneisen tensor (Angel *et al.*, 2019; Murri *et al.*, 2019). The strains can then be used to determine the P_{inc} applying the ambient-pressure elastic tensor of quartz, such as the one provided by Wang *et al.* (2015). Considering this renewed interest in the response of the Raman spectrum of quartz to compression, a detailed characterization is necessary. In fact, most recent studies are focused on the two most intense peaks, and the dependence of the polar modes wavenumbers on the orientation of the sample with respect to the direction of the incident and scattered light (Shapiro & Axe, 1972) has been poorly described. While a free single crystal can be easily oriented, this is not the case for an inclusion, trapped within the host, and this might be an issue for elastic geobarometry methods since the Grüneisen parameters were calculated for the transverse optic (TO) E modes and not for the longitudinal optic (LO) E modes, that are measured experimentally in some orientations. Similar considerations can be applied to response of quartz to heating, where it is also important to characterize the α - β phase transition.

The pressure dependence of the polarized Raman scattering of quartz was studied under hydrostatic conditions up to 9 GPa. This allowed to extend the available pressure calibrations to a larger number of modes, providing polynomial functions that describe the relationship between pressure P and wavenumber shift $\Delta\omega$ for the 128-, 206-, 265-, 464-, 696-, 809-, 1080- and 1161- cm^{-1} modes. It is also shown that the measured pressure dependence of all of the Raman shifts of quartz is predicted by the phonon-mode Grüneisen tensors up to 2 GPa, thus validating the parameter values calculated by Murri *et al.* (2019). The pressure behavior of the LO-TO splitting was also characterized. The pressure induced wavenumber changes and derived phonon compressibilities show that longitudinal and transverse modes can be used interchangeably for the calculation of strains through the Grüneisen tensor. This is an important information for the practical use of Raman geobarometry, because it experimentally supports the application of the Grüneisen-tensor approach (Angel *et al.*, 2019; Murri *et al.*, 2019) to both LO and TO modes and verifies that the orientation of quartz inclusions with respect to the surface of the host does not introduce bias for the E modes. A thorough inspection of the linewidths as a function of pressure shows that they are sensitive to the metastability of the quartz structure with respect to the high-pressure silica polymorphs, suggesting that strong multiphonon interactions contribute to the stability of the structure of quartz at ambient conditions.

At ambient pressure, quartz undergoes a well known phase transition at 573 °C from the low-temperature α -phase to the high temperature β -phase. The two phases crystallize in the chiral space groups $P3_121$ and $P3_221$, and $P6_222$ and $P6_422$, respectively (Donnay & Le Page, 1978). Theoretically, only one A_1 mode, the 464-cm⁻¹ mode, out of the four existing in quartz is allowed to persist in the β -phase. However, the 206-cm⁻¹ A_1 mode is present after the transition from the α to the β phase. This mode is the most sensitive to temperature and has often been considered as the soft-mode driving the phase transition. However, the huge temperature dependence and anomalous broadening of this mode have been shown to be related to another spectral feature centered around 147 cm⁻¹ at ambient conditions that is a two-phonon excitation (Scott, 1968; 1974) whose phonon wave-number tends to zero approaching the phase transition. Scott (1968) suggested that these two spectral features could interact via Fermi resonance and that at room and intermediate temperatures, the fundamental A_1 mode and the A_1 -symmetry two-phonon band are mixed. Above the transition temperature, the excitation has predominately a second-order character and thus does not violate selection rules. The other modes in quartz obey the selection rules and the remaining two A_1 modes disappear at the phase transition. The Grüneisen tensor components calculated by Murri *et al.* (2019) were tested against experimental wavenumber shifts as a function of temperature using the unit-cell parameters from Carpenter *et al.* (1998) and those calculated from the equation of state of quartz by Angel *et al.* (2017). The modes at 128 and 206 cm⁻¹ have Grüneisen tensor components greater than 1 and show a poor agreement with the predictions, whereas the other two modes have Grüneisen tensor components around 0.5 and show a good agreement, as already described in Murri *et al.* (2019).

The information collected from the experiments at high pressure and high temperature on the free quartz crystal were used to interpret the Raman scattering from an actual quartz inclusion in garnet at high temperature. The major effect of the confinement of the quartz crystal in the host during the heating is the absence of the α - β phase transition. This is not surprising, since the stress imposed on the sample is expected to shift the transition point to higher temperature. The absence of the phase transition is confirmed by the temperature dependence of the peak position and Full width at half maximum (FWHM), as shown in Fig. 1, where the data from the free quartz crystal are also reported for comparison. All Raman modes of the inclusion, except the A_1 mode at 355 cm⁻¹, which is a hard mode and thus less sensitive to pressure and temperature (Hemley, 1987; Salje *et al.*, 1992), have higher wavenumbers than the modes from the free quartz at the same temperature, confirming that the inclusion remains under pressure over the entire temperature range of the measurements. From the variation of the peak positions with respect to temperature for the modes at 464 and 206 cm⁻¹ it is possible to identify different regimes. The first regime is characterized by linear variation for both the free crystal and the inclusion peak positions, since they are both in the α -phase. However, the linear trends of the 464- and 206-cm⁻¹ modes have a different slope, because of the confinement of the inclusion. Approaching the transition, the data from the free quartz show the expected behavior: a minimum in the peak position that corresponds to a maximum in the FWHM. In the case of the quartz inclusion the peak positions are instead clustered around a constant value. Whereas the pre-transition and transition effects are clearly visible in the free quartz data, this is not the case for the inclusion data. Models based on isotropic stress are not able to reproduce the experimental data from the inclusion. The disagreement could be due to different effects. One first effect to consider is the dependence of $(\partial\omega/\partial P)$ upon temperature. However, Schmidt & Ziemann (2000) could determine a constant isotherm slope, at least for the 464-cm⁻¹ mode. Another possible cause of disagreement between the model and the experimental data might be the composition of the garnet. However, the difference between the P_{inc} and the resulting shifts for different endmembers is small. Additionally, temperature-induced changes in the host can be excluded. In fact, up to 1000 K the most intense peak of garnet, the A_{1g} mode at ~ 920 cm⁻¹, shows the expected behavior with the peak position decreasing linearly upon heating (Gillet *et al.*, 1992).

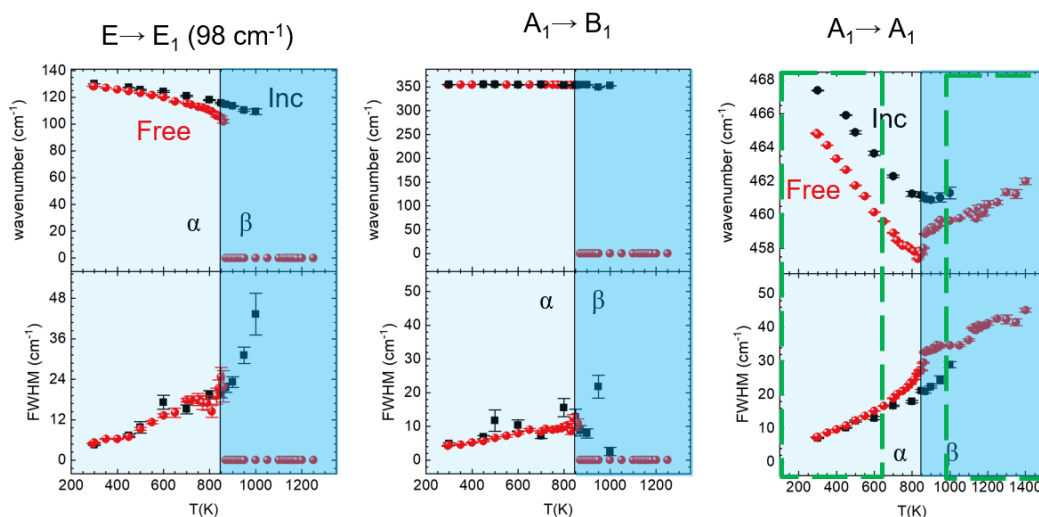


Fig. 1 - Temperature dependence of the peak positions of selected modes for a free and trapped quartz.

When heating from 1000 to 1050 K, the sample unexpectedly jumped and it was not possible to continue the measurement. The sample was cooled down to room temperature and heated again, but in this second run the sample jumped at 1150 K and broke into pieces; it was possible to recover only a fragment of the garnet host. The spectra at room temperature before the two heating runs show that the host-inclusion system was not altered by the first heating, while the recovered garnet after the second run has a distinctly different spectrum with additional peaks attributed to nanocrystalline hematite. In the recovered fragment, the most intense peak in the garnet host is shifted from $920.05(3) \text{ cm}^{-1}$ to $918.07(7) \text{ cm}^{-1}$, reflecting the oxidation of Fe^{+2} to Fe^{+3} . This effect might be the result of the difference in elastic properties upon heating of the two members of the pair, in particular, when the quartz inclusion approaches the phase transition, that is hindered by the confinement within the host, resulting in the jump and breakage of the system.

An example of application of elastic geobarometry is the determination of the conditions of elastic equilibration in a quartz in garnet from eclogite xenoliths hosted in Yakutian kimberlites (Russia). The inclusion pressure or strain were derived from X-ray diffraction and Raman measurements, were corrected for the effects of mutual relaxation between the inclusion and the host, and then used, together with the known variation of the unit cell parameters of quartz with pressure and temperature, to calculate a line of possible entrapment conditions from each of the corrected strains along a and c crystallographic axes. The intersection of these two lines provides a unique P and T of entrapment and /or equilibration for each inclusion, three of which are very similar and close to 3 GPa, showing that trapped in garnet can persist when the rock reaches the stability field of coesite, This result not only supports a metamorphic origin for these xenoliths, but also show that interpreting P and T conditions reached by a rock from the simple phase identification of key inclusion minerals can be misleading.

REFERENCES

- Alvaro, M., Mazzucchelli, M.L., Angel, R.J., Murri, M., Campomenosi, N., Scambelluri, M., Nestola, F., Korsakov, A., Tomilenko, A.A., Marone, F., Morana, M. (2020): Fossil subduction recorded by quartz from the coesite stability field. *Geology*, **48**, 24-28.
- Angel, R.J., Alvaro, M., Miletich, R., Nestola, F. (2017): A simple and generalised P-T-V EoS for continuous phase transitions, implemented in EosFit and applied to quartz. *Contrib. Mineral. Petr.*, **172**(5), 29.
- Angel, R.J., Murri, M., Mihailova, B., Alvaro, M. (2019): Stress, strain and Raman shifts. *Z. Krist.-Cryst. Mater.*, **234**, 129-140.
- Bonazzi, M., Tumiati, S., Thomas, J.B., Angel, R.J., Alvaro, M. (2019): Assessment of the reliability of elastic geobarometry with quartz inclusions. *Lithos*, **350-351**, 105201.

- Carpenter, M.A., Salje, E.K.H., Graeme-Barber, A., Wruck, B., Dove, M.T., Knight, K.S. (1998): Calibration of excess thermodynamic properties and elastic constant variations associated with the $\alpha \leftrightarrow \beta$ phase transition in quartz. *Am. Mineral.*, **83**, 2-22.
- Donnay, J.D.H. & Le Page, Y. (1978): The Vicissitudes of the Low-Quartz Crystal Setting or the Pitfalls of Enantiomorphism. *Acta Crystallogr. A*, **34**, 584-594.
- Enami, M., Nishiyama, T., Mouri, T. (2007): Laser Raman microspectrometry of metamorphic quartz: A simple method for comparison of metamorphic pressures. *Am. Mineral.*, **92**, 1303-1315.
- Gillet, P., Fiquetw, G., Malézieux, J.M., Geiger, C.A. (1992): High-pressure and high-temperature Raman spectroscopy of end-member garnets: pyrope, grossular and andradite. *Eur. J. Mineral.*, **4**, 651-664.
- Glinnemann, J., King, H.E., Schulz, H., Dacol, F. (1992): Crystal structures of the low-temperature quartz-type phases of SiO₂ and GeO₂ at elevated pressure. *Z. Krist-Cryst. Mater.*, **198**, 177-212.
- Gonzalez, J.P., Thomas, J.B., Baldwin, S.L., Alvaro, M. (2019): Quartz-in-garnet and Ti-in-quartz thermobarometry: Methodology and first application to a quartzfeldspathic gneiss from eastern Papua New Guinea. *J. Metamorph. Geol.*, **37**, 1193-1208.
- Hemley, R.J. (1987): Pressure dependence of Raman spectra of SiO₂ polymorphs: α -quartz, coesite, and stishovite. In: "High-Pressure Research in Mineral Physics: A Volume in Honor of Syun-iti Akimoto", M.H. Manghnani & Y. Syono, eds. *Geophys. Monograph Ser.*, **39**, 347-359.
- Ikuta, D., Kawame, N., Banno, S., Hirajima, T., Ito, K., Rakovan, J.F., Downs, R.T., Tamada, O. (2007): First in situ X-ray identification of coesite and retrograde quartz on a glass thin section of an ultrahigh-pressure metamorphic rock and their crystal structure details. *Am. Mineral.*, **92**, 57-63.
- Mazzucchelli, M.L., Reali, A., Morganti, S., Angel, R.J., Alvaro, M. (2019): Elastic geobarometry for anisotropic inclusions in cubic hosts. *Lithos*, **350-351**, 105218.
- McCammon, C., Hutchison, M., Harris, J. (1997): Ferric iron content of mineral inclusions in diamonds from São Luiz: A view into the lower mantle. *Science*, **278**, 434-436.
- Milani, S., Nestola, F., Angel, R.J., Nimis, P., Harris, J.W. (2016): Crystallographic orientations of olivine inclusions in diamonds. *Lithos*, **265**, 312-316.
- Miyahara, M., Ohtani, E., El Goresy, A., Lin, Y., Feng, L., Zhang, J.-C., Gillet, P., Nagase, T., Muto, J., Nishijima, M. (2015): Unique large diamonds in a ureilite from Almahata Sitta 2008 TC3 asteroid. *Geochim. Cosmochim. Ac.*, **163**, 14-26.
- Murri, M., Mazzucchelli, M.L., Campomenosi, N., Korsakov, A.V., Prencipe, M., Mihailova, B.D., Scambelluri, M., Angel, R.J., Alvaro, M. (2018): Raman elastic geobarometry for anisotropic mineral inclusions. *Am. Mineral.*, **103**, 1869-1872.
- Murri, M., Alvaro, M., Angel, R.J., Prencipe, M., Mihailova, B.D. (2019): The effects of non-hydrostatic stress on the structure and properties of alpha-quartz. *Phys. Chem. Miner.*, **46**, 487-499.
- Nabiei, F., Badro, J., Dennenwaldt, T., Oveisi, E., Cantoni, M., Hébert, C., El Goresy, A., Barrat, J.-A., Gillet, P. (2018): A large planetary body inferred from diamond inclusions in a ureilite meteorite. *Nat. Commun.*, **9**, 1327.
- Nestola, F., Nimis, P., Angel, R.J., Milani, S., Bruno, M., Prencipe, M., Harris, J.W. (2014): Olivine with diamond-imposed morphology included in diamonds. Syngensis or protogenesis? *Int. Geol. Rev.*, **56**, 1658-1667.
- Nimis, P., Angel, R.J., Alvaro, M., Nestola, F., Harris, J.W., Casati, N., Marone, F. (2019): Crystallographic orientations of magnesiochromite inclusions in diamonds: what do they tell us? *Contrib. Mineral. Petr.*, **174(4)**, 29.
- Piazzini, M., Morana, M., Coisson, M., Marone, F., Campione, M., Bindi, L., Jones, A.P., Ferrara, E., Alvaro, M. (2019): Multi-analytical characterization of Fe-rich magnetic inclusions in diamonds. *Diam. Relat. Mater.*, **98**, 107489.
- Salje, E.K.H., Ridgwell, A., Guttler, B., Wruck, B., Dove, M.T., Dolino, G. (1992): On the displacive character of the phase transition in quartz: a hard-mode spectroscopy study. *J. Phys-Condens. Mat.*, **4**, 571-577.
- Schmidt, C. & Ziemann, M.A. (2000): In-situ Raman spectroscopy of quartz: A pressure sensor for hydrothermal diamond-anvil cell experiments at elevated temperatures. *Am. Mineral.*, **85**, 1725-1734.
- Scott, J.F. (1968): Evidence of Coupling Between One- and Two-Phonon Excitations in Quartz. *Phys. Rev. Lett.*, **21**, 907-910.
- Scott, J.F. (1974): Soft-mode spectroscopy: Experimental studies of structural phase transitions. *Rev. Mod. Phys.*, **46**, 83-128.
- Shapiro, S.M. & Axe, J.D. (1972): Raman Scattering from Polar Phonons. *Phys. Rev. B*, **6**, 2420-2427.
- Stachel, T. & Harris, J.W. (2008): The origin of cratonic diamonds - Constraints from mineral inclusions. *Ore Geol. Rev.*, **34**, 5-32.
- Stachel, T., Harris, J.W., Brey, G.P. (1998): Rare and unusual mineral inclusions in diamonds from Mwadui, Tanzania. *Contrib. Mineral. Petr.*, **132**, 34-47.
- Wang, J., Mao, Z., Jiang, F., Duffy, T.S. (2015): Elasticity of single-crystal quartz to 10 GPa. *Phys. Chem. Miner.*, **42**, 203-212.
- Woodland, A.B. & Angel, R.J. (2000): Phase relations in the system fayalite-magnetite at high pressures and temperatures. *Contrib. Mineral. Petr.*, **139**, 734-747.